THE UNIVERSITY OF MICHIGAN

COLLEGE OF ENGINEERING
Department of Engineering Mechanics
Department of Mechanical Engineering
Tire and Suspension Systems Research Group

Translation No. 5

MECHANICS OF THE BELTED TIRE

F. Böhm

translated by

Eugen Füner

Project Director: S. K. Clark

ORA Project 02957

administered through:

OFFICE OF RESEARCH ADMINISTRATION ANN ARBOR

February 1967

engn

UMR0420

The original was published in Ingeniur-Archiv, XXXV, 1966.

The Tire and Suspension Systems Research Group
at The University of Michigan is sponsored by:

FIRESTONE TIRE AND RUBBER COMPANY

GENERAL TIRE AND RUBBER COMPANY

B. F. GOODRICH TIRE COMPANY

GOODYEAR TIRE AND RUBBER COMPANY

UNIROYAL, INC.

MECHANICS OF THE BELTED TIRE

F. Böhm

Summary: The ring on an elastic foundation is the basic concept to formulate the static and dynamic properties of radial cord tires. To illustrate the theory, static axial deflection under concentrated load, natural frequencies of radial vibrations and the formation of stationary waves at high rolling speeds are treated. By comparing measurements of radial and axial vibrations with theoretical results it is shown that the model in question may well be used.

1. Introduction. In 1948 the Michelin Tire Company developed a tire which differed in its design from the usual bias ply tire (Fig. 1). The sidewall cords (a) reinforcing the rubber run in radial planes, so that this tire is called a radial tire. It is also called a belted tire since the tread of this tire is reinforced by a steel-cord reinforced belt (b). The innermost belt ply (ply 1) is in direction almost parallel to the radial cords. Both outer layers (plies 2 and 3) have a direction of ±18° measured from the centerline of the tire. Ply 1 acts as a foundation layer for the two others and is not utilized in all belted tire designs. The internal pressure causes a considerable tension in the longitudinal direction of the belt. For a given cross section this is easily found. Although the belt itself is relatively stiff, the sidewalls are very flexible and the cross section due to internal pressure can be determined by use of membrane equilibrium. The belt can be considered as a stiff body elastically supported on the radially reinforced membrane. Experiments by Hinton [1] and Borgmann [2] show that the deflections of a belt are similar to those of a ring on an elastic foundation. The same conclusion is reached by Frank [3] in his dissertation. The ring on

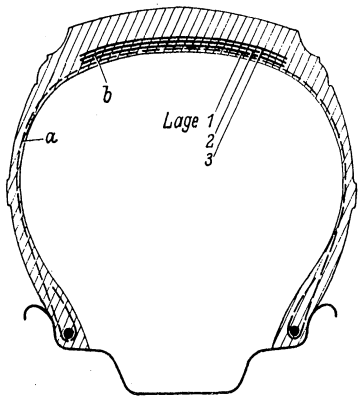

Fig. 1. Cross section of a belted automobile tire. a-radial reinforcement, b-belt (steel-cord reinforced). Ply 1 is parallel to (a), plies 2 and 3 are reinforced at an angle of $\beta=\pm 18°$ from the circumferential direction.

elastic foundation was treated by Federhofer [4], Volterra [5], and Rodriguez [6]. For the derivation of the equations of motion one must consider the equilibrium of the deformed belt element, because of the pretension in the belt. Nonlinear terms will be neglected. It is the purpose of this paper to discuss the linearly elastic properties of deformation, vibration, and rolling.

2. Mechanical Properties of the Belt. In order to treat the belted tire as a ring on an elastic foundation, the properties of the belt have to be determined first. The internal stresses caused by tension and bending of the belt are obviously carried by the steel cords. At the edges of the belt, however, the cord forces must of necessity drop to zero, and hence they have to be transmitted to other cord layers. Thus, large shear stresses take place at the belt edge, especially in the rubber layers between the two oblique plies.

In order to illustrate these internal properties of the belt, the deformations have been studied using a model made of foam rubber.[1] Figure 2 shows the design of the three-layer belt. The oblique reinforcement was made by cementing threads on the foam, whereas the transverse reinforcement was obtained by cementing rattan strips to the outside in order to support compression forces. Because of the longitudinal force T and the distance between the layers d an unbalanced torque arises.

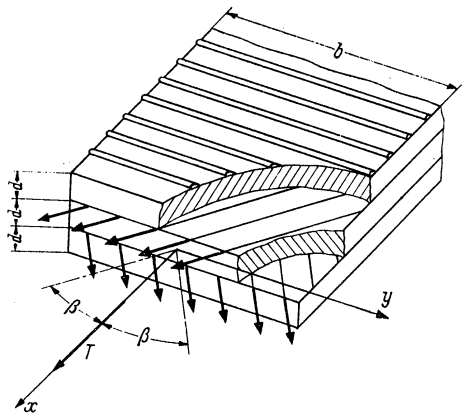

Fig. 2. Belt model (foam rubber).

$$T_M = \frac{1}{2} T d \tan \beta . \tag{2.1}$$

The tension force in the belt T is made up of T_0, which is determined by the internal pressure of the tire, and by a part which is dependent upon the longitudinal strain ϵ of the belt. The term (EF) is an effective stiffness,

[1] G. Höfer, Diplomarbeit, accepted by the "Fakultät für Bauwesen der TH Stuttgart, Lehrstuhl I für Techn. Mechanik," 1965.

or product of modulus and area,

$$T = T_0 + (EF)\,\varepsilon\,. \tag{2.2}$$

Figure 3 shows the belt model in tension. Because of T_M the free edge is noticeably twisted. The shear deformation of the rubber layers along the belt edge are shown in Fig. 4. Since the layer which is reinforced with rattan strips is located d and 2d respectively from the oblique reinforcements, and since there is a transverse contraction as a result of the longitudinal tension, the cross section shows a bending effect. This can be seen on the bright lines in Fig. 4. The shear deformation can be made visible, and for this purpose one inserts needles into the rubber layer. Figure 5 shows a plan view of the belt. A wool thread was pulled through the eyes of the needles which makes the shear deformation across the width of the belt visible. The wooden bars to the right and left of the row of needles hinder the above-mentioned warping of the cross section. There are other shear deformations too, but they are smaller and dependent upon the variable transverse contractions of the different reinforced plies. For example one can see in Fig. 5 that the needles are slightly tipped towards the middle of the belt.

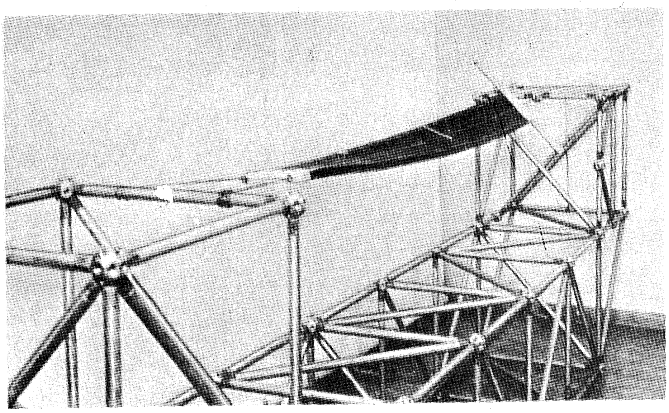

Fig. 3. Deformation of the belt model in tension.

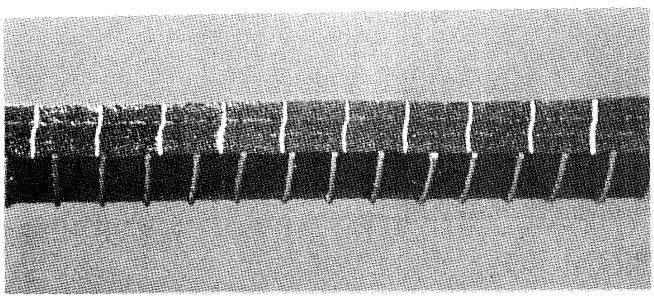

Fig. 4. Shear deformation of the middle rubber layer along the edge of the belt.

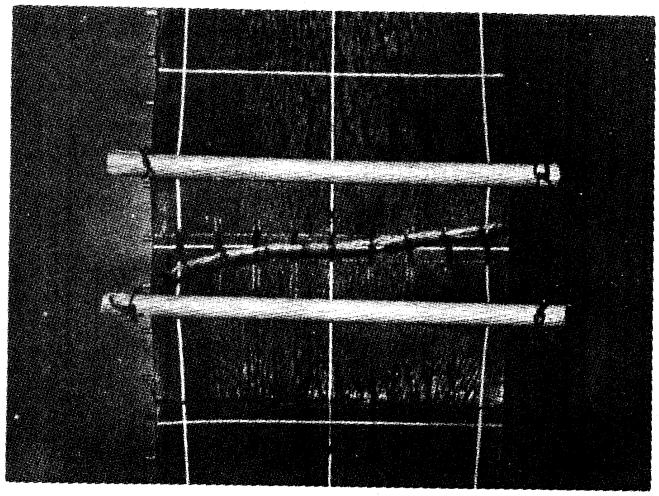

Fig. 5. Shear deformation of the middle rubber layer across the width of the belt. It is made visible by needles which are inserted into the rubber and strung with woolen yarn.

If one omits the transverse reinforcement one gets, for the same longitudinal extension, a completely analogous shear deformation of the middle layer. The transverse contraction occurs here only in the rubber layer in the middle. An originally plane section of the belt has after deformation the form shown in Fig. 6. This somewhat simpler behavior is treated analytically in the following.

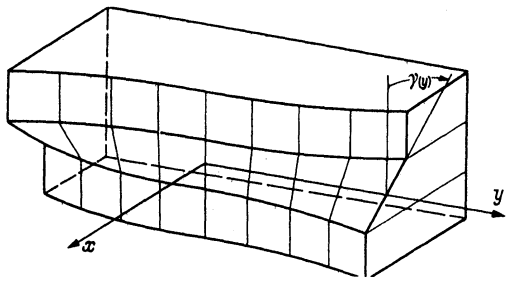

Fig. 6. Graph of the deformation of the cross section without transverse reinforcement.

The field of deformations is approximated by the simple expression:

$$\mathfrak{z} = \begin{Bmatrix} u(x) \pm \frac{d}{2}\gamma(y) \\ v(y) \end{Bmatrix} \tag{2.3}$$

Because of the shear deformation in the x-direction the threads are unloaded towards the edge and this results in a variable transverse contraction in the y-direction. These effects, however, occur only in the immediate vicin-

ity of the edge. They show up strongly only with the belt model, since the foam rubber has a very small shear modulus.

We consider the belt to be at first loaded by T_0 and uniformly strained by the amount $|\varepsilon_{0x}| \ll 1$, and having the transverse contraction $|\varepsilon_{0y}| \ll 1$. The strain ε_{0f} of the steel cords is given by

$$\varepsilon_{0f} = \varepsilon_{0x} \cos^2\beta + \varepsilon_{0y} \sin^2\beta \,. \tag{2.4}$$

The strain energy of the belt per "unit" length is

$$\Phi = \int_{-\frac{b}{2}}^{+\frac{b}{2}} \left\{ \frac{1}{2} E_G \frac{3\,d}{1-\nu_G^2} \left[(\varepsilon_{0x}^2 + \varepsilon_{0y}^2) + 2\,\nu_G\,\varepsilon_{0x}\,\varepsilon_{0y} \right] + E_f\, n_y \frac{1}{\cos\beta} \varepsilon_{0f}^2 \right\} dy \,,$$

where E_f is the modulus of the cord, n_y is the end count of wires across a section in the y-direction, E_G is Young's modulus and ν_G is Poisson's ratio for rubber. The virtual work due to the external force T_0 is $\delta' A = T_0 \delta\varepsilon_{0x}$, and therefore is

$$\delta' A = \delta\Phi = \frac{\partial\Phi}{\partial\varepsilon_{0x}} \delta\varepsilon_{0x} + \frac{\partial\Phi}{\partial\varepsilon_{0y}} \delta\varepsilon_0 \,.$$

Calling the end count of cords n, this yields

$$\left.\begin{aligned} E_G \frac{3\,d}{1-\nu_G^2} (\varepsilon_{0x} + \nu_G\,\varepsilon_{0y}) + E_f\, n \left[\frac{1}{2} (1 + \cos 2\beta)^2 \varepsilon_{0x} + \frac{1}{2} (\sin 2\beta)^2 \varepsilon_{0y} \right] &= \frac{T_0}{b} \\ E_G \frac{3\,d}{1-\nu_G^2} (\varepsilon_{0y} + \nu_G\,\varepsilon_{0x}) + E_f\, n \left[\frac{1}{2} (\sin 2\beta)^2 \varepsilon_{0x} + \frac{1}{2} (1 - \cos 2\beta)^2 \varepsilon_{0y} \right] &= 0 \,. \end{aligned}\right\} \tag{2.5}$$

These equations have already been derived by F. Martin [7] in a different way.

If the strain of the threads ε_{0f} is neglected in the strain energy, one obtains a relationship between the strains ε_{0x} and ε_{0y}:

$$\varepsilon_{0f} = 0 = \varepsilon_{0x} \cos^2\beta + \varepsilon_{0y} \sin^2\beta \,. \tag{2.6}$$

From (2.5) follows

$$E_G \frac{3\,d\,b}{1-\nu_G^2} \left[1 - \frac{2\,\nu_G}{\tan^2\beta} + \frac{1}{\tan^4\beta} \right] \varepsilon_{0x} = (EF)\,\varepsilon_{0x} = T_0 \,, \tag{2.7}$$

where (EF) can be called the effective stiffness for tension.

From Eqs. (2.7) and (2.6) ε_{0x} and ε_{0y} can be determined. Now we look at the edge disturbance of this fundamental condition. Let

$$\varepsilon_x = \frac{\partial u}{\partial x} = \varepsilon_{0x}\,, \qquad \varepsilon_y = \frac{\partial v}{\partial y} = \varepsilon_{0y} + \varepsilon_y(y)\,, \qquad \gamma_{xy} = \pm\frac{d}{2}\frac{\partial \gamma}{\partial y} = \pm\frac{d}{2}\gamma'(y)\,. \tag{2.8}$$

Since the cords are unloaded near the boundary one has to take their strain into account:

$$\varepsilon_f = \varepsilon_{0f} - \frac{d}{2}\sin\beta\cos\beta\,\gamma'(y) + \sin^2\beta\,\varepsilon_y(y)\,. \tag{2.9}$$

On the edge of the belt ε_f has to vanish. We write the strain energy

$$\Phi = \int_{-b/2}^{+b/2}\left\{\frac{1}{2}E_G\frac{3d}{1-\nu_G^2}\left[\varepsilon_{0x}^2 + (\varepsilon_{0y}+\varepsilon_y)^2 + 2\nu_G\,\varepsilon_{0x}(\varepsilon_{0y}+\varepsilon_y)\right] + E_f\,n\,\varepsilon_f^2 + \frac{1}{2}dG\gamma^2\right\}dy\,. \tag{2.10}$$

Because of the additional degrees of freedom, γ and ε_y, Φ_{min} is now smaller than without boundary effects. We keep ε_{ox} and ε_{oy} fixed and take a variation such, that $\Phi(\gamma,\gamma',\varepsilon_y)$ becomes a minimum value. If we represent the integrand in brackets by F, the Euler equations become:

$$\frac{\partial F}{\partial \varepsilon_y} = 0\,, \qquad \frac{\partial F}{\partial \gamma} - \frac{\partial}{\partial y}\left(\frac{\partial F}{\partial \gamma'}\right) = 0\,. \tag{2.11}$$

These conditions yield:

$$\frac{1}{2}E_G\frac{3d}{1-\nu_G^2}(2\varepsilon_{0y} + 2\varepsilon_y + 2\nu_G\varepsilon_{0x}) + 2E_f\,n\left(\varepsilon_{0f} - \frac{d}{2}\sin\beta\cos\beta\gamma' + \varepsilon_y\sin^2\beta\right)\sin^2\beta = 0\,, \tag{2.12}$$

$$-\left(\frac{d}{2}\sin\beta\cos\beta\right)^2 2E_f\,n\,\gamma'' + dG\gamma + 2E_f\,n\frac{d}{2}\sin^3\beta\cos\beta\,\varepsilon_y' = 0\,. \tag{2.13}$$

Equation (2.12) relates γ' and ε_y. The zero strain of the cords along the edge and the condition that the transverse tension of the rubber body vanishes serve as boundary conditions:

$$E_G\frac{3d}{1-\nu_G^2}(\varepsilon_{0y} + \varepsilon_y|_{y=\pm b/2} + \nu_G\varepsilon_{0x}) = 0\,. \tag{2.14}$$

By substituting into (2.12) we get $\varepsilon_f = 0$! From (2.14) we determine

$$\varepsilon_y|_{y=\pm b/2} = -\varepsilon_{0y} - \nu_G\varepsilon_{0x}\,, \tag{2.15}$$

and get from (2.12) using (2.4)

$$\gamma'|_{y=\pm b/2} = \frac{2\varepsilon_{0x}}{d}(\cot\beta - \nu_G\tan\beta) = \gamma_r'\,. \tag{2.16}$$

Differentiation of (2.12) yields

$$\varepsilon_y' = \frac{2E_f n\frac{d}{2}\sin^3\beta\cos\beta\,\gamma''}{E_G\frac{3d}{1-\nu_G^2} + 2E_f n\sin^4\beta}\,,$$

and because of the large stiffness of the steel-cord layer compared with the rubber layer we get

$$\varepsilon_y' \doteq \frac{2}{d} \cot \beta \left(1 - \frac{E_G \frac{3\,d}{1-\nu_G^2}}{2\,E_f\, n \sin^4 \beta} \right). \tag{2.17}$$

We substitute Eq. (2.17) into Eq. (2.13) and get finally a second order ordinary differential equation for the shear deformation

$$- E_G \frac{(3\,d)^2}{1-\nu_G^2} \cot \beta \frac{d}{2} \gamma'' + dG\gamma = 0\,. \tag{2.18}$$

The solution is an exponential function (γ_r'/λ) exp $(-\lambda_y)$ where y is measured now from the boundary. The decay-factor is

$$\lambda = \sqrt{\frac{G \tan \beta}{\frac{1}{2} E_G \frac{9\,d^2}{1-\nu_G^2}}} = \frac{1}{3\,d} \sqrt{(1-\nu_G) \tan \beta}\,. \tag{2.19}$$

For practical numerical values (ν_G = .5, d = .17 cm, β = 18.5°) one obtains λ = 1.36 cm^{-1}. The subtangent to the curve $\gamma(y)$ at the edge of the belt therefore has the length 0.73 cm and represents the region of influence of the shear deformation. Undoubtedly the above equations of deformation are only an approximate description. An accurate treatment would include a two-dimensional deformation-problem and would be too lengthy for this paper.

Now one may elucidate the important properties of the force distribution in the laminated medium under tension. The tension T_0 is transmitted by the oblique cords, but in a narrow zone along the edge it is attenuated. It is reduced by shear deformation γ of the intermediate layer, and by the transverse contraction ε_y of the rubber in all three layers, which is approximately constant through the thickness.

In Fig. 7 a construction with transverse reinforcement is shown. The transverse reinforcement resists the tendency for the belt to contract laterally. This is brought about by a shear deformation 1/2 $\delta(y)$ and $\delta(y)$ respectively, as shown in Fig. 7. A procedure analogous to the one used above yields

$$\varepsilon_{0x} = \frac{T_0}{2\,b\,E_f\,n \cos^4 \beta} \cdot \frac{1 + \sin^4 \beta}{1 - \cos 2\beta \sin^4 \beta}\,, \tag{2.20}$$

$$\varepsilon_{0y} = - \varepsilon_{0x} \frac{2 \sin^2 \beta \cos^2 \beta}{1 + 2 \sin^4 \beta}\,. \tag{2.21}$$

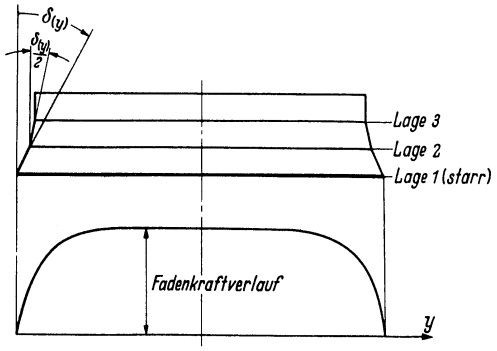

Fig. 7. Shear deformation in y-direction of a ring with rigid restraint at the base.

We introduce for both oblique cords an average cord strain

$$\varepsilon_f = \varepsilon_{0f} - \frac{d}{2}\sin\beta\cos\beta\,\gamma' - 1.25\,d\sin^2\beta\,\delta' \tag{2.22}$$

and in the expression for the elastic strain energy we use only the strain energy of the oblique cords and the shear energy of the intermediate layers. With this we can find a differential equation for X(y) where

$$X(y) = \frac{d}{2}\sin\beta\cos\beta\,\gamma(y) + 1.25\,d\sin^2\beta\,\delta(y); \tag{2.23}$$

analogous to (2.18)

$$-2\,n\,E_f\left[\left(\frac{d}{2}\sin\beta\cos\beta\right)^2 + \left(1.25\,d\sin^2\beta\right)^2\right]X'' + dG\,X = 0 \tag{2.24}$$

The solutions are:

$$\gamma(y) = \frac{d}{2}\sin\beta\cos\beta\,\lambda\,\frac{2\,n\,E_f}{G\,d}\,\varepsilon_{0f}\,e^{-\lambda y}, \qquad \delta(y) = 1.25\,d\sin^2\beta\,\lambda\,\frac{2\,n\,E_f}{G\,d}\,\varepsilon_{0f}\,e^{-\lambda y}. \tag{2.25}$$

The decay-constant λ is given by

$$\lambda = \sqrt{\frac{G\,d}{2\,n\,E_f\left[\left(\frac{d}{2}\sin\beta\cos\beta\right)^2 + (1.25\sin^2\beta)^2\right]}} \tag{2.26}$$

Given E = 1.8x10 kp/cm^2 (cord), F = .253x10^{-2}cm^2, n = 6.5 cm^{-1}, G = 50 kp/cm^2 β = 17.5°, and d = .18 cm. With these values λ = .45 cm^{-1} and the subtangent has the length 2.2 cm. Calculating the effectiveness of the belt one will subtract Δb from the width of the belt and using this new quantity

$$b^* = b - \Delta b = b - \frac{1{,}4}{\lambda} \tag{2.27}$$

which subtracts the influence of the boundary.

As a good approximation for small angles β we obtain for the effective stiffness (EF) of the belt with foundation

$$(EF) = 2\, E_f\, n\, b^*\, \cos^4\beta\,, \tag{2.28}$$

while for the bending stiffness

$$(EI_x) = 2\, E_f\, n\, \frac{b^{*3}}{12}\, \cos^4\beta\,, \tag{2.29}$$

and the bending stiffness in the orthogonal direction

$$(EI)_y = (EI_x)\, \frac{3\, d^2}{b^{*2}} + E_G\, \frac{b\, t^3}{12} \tag{2.30}$$

is obtained by proportioning according to the second power of radius of gyration and adding the bending effect of the rubber. In torsion the effect of the cross sectional portion of the rubber is practically the only effect. Therefore we have:

$$(GI_p) = G\left(\frac{b\, t^3}{12} + \frac{b^3\, t}{12}\right). \tag{2.31}$$

Hence the belt has been reduced to a beam in its external mechanical action. But there are also effects which cannot be explained this way. Although the flattening of the belt in the contact region of the tire requires only small displacement, it illustrates the limits of the beam model of the belt.

We investigate now the effect of the cord reinforcement under bending about the y-axis of the belt section. Due to the thickness of the layers we have a strain difference $\Delta\varepsilon = d \cdot \kappa$ between the cords in the two oblique directions. In Fig. 8 we examine an element of the belt. Along the edges we obtain transverse forces which are unbalanced because of the difference in strain.

$$Q = \overbrace{2\, E_f\, n\, b^*\, \cos^3\beta\, \sin\beta}^{\nu}\, \Delta\varepsilon = \nu \cdot d \cdot \varkappa\,, \tag{2.32}$$

Later on in Section 4, Eq. (4.4) the change in curvature will be given.

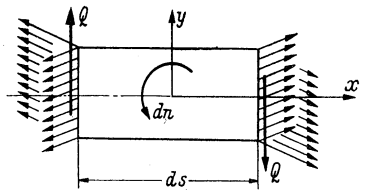

Fig. 8. Transverse forces Q caused by bending about the y-axis.

The result is then a distributed moment which acts as a small disturbance on the belt:

$$n = -Q = -\nu d \frac{v'' + v}{a^2}. \tag{2.33}$$

The curvature of the section, $1/\rho_G$ (Fig. 9), which is very small in general, vanishes in the area of contact caused by the flattening. The transition to the curvature $1/\rho_G$ in some distance from the area of contact is not given by this theory of the belted tire. If one knows $\rho_G(\Phi)$, by measurement or any reasonable assumption then there acts as a disturbing moment on the belt

$$n = -\nu d \frac{1}{\varrho_G(\varphi)}. \tag{2.34}$$

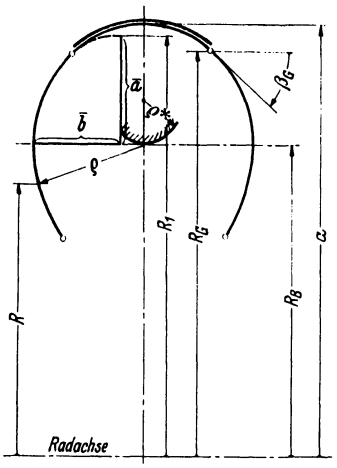

Fig. 9. Notation for the dimensions of a section of a belted tire.

3. The Shape of the Side Walls in Equilibrium and the Spring Rates of the Belt. The equilibrium shape of the cross section of a cord reinforced, axisymmetric membrane has been treated by Day and Gehman [8]. For radial reinforcements one obtains solutions in terms of elliptic functions. One can show that the radius of curvature ρ (Fig. 9) satisfies the equation

$$\varrho = \frac{R_1^2 - R_B^2}{2R} \tag{3.1}$$

The value of ρ varies only slightly within the region of interest. Thus the outer part of the cross section can be represented closely by an ellipse, and the inner part by an involute of a circle. The semiaxes of the ellipse are given by

$$\bar{a} = R_1 - R_B \tag{3.2}$$

and

$$\bar{b} = (R_1 - R_B)\sqrt[3]{\frac{R_B}{R_1}}. \tag{3.3}$$

The base circle of the matching circular involute is given by

$$\varrho^* = \frac{(R_1^2 - R_B^2)^2}{4\,R_B^3}. \tag{3.4}$$

If the shape of the cross section is fixed, the tension in the belt can easily be determined. From Fig. 9 we get

$$T_0 = p\,b\,R_G - p\,(R_G^2 - R_B^2)\tan\beta_G\,.$$

The angle β_G in general is very small such that one can assume without much error

$$T_0 = p\,b^*\,a \tag{3.5}$$

For a real tire the shape in equilibrium deviates only slightly from a circle. For the determination of the stiffnesses of the belt we restrict ourselves to the concept developed by Rotta [9], for a cylindrical tire-element, i.e., we neglect the circumferential curvature of the membrane. Rotta showed that the lateral stiffness k_S (Fig. 10a) satisfies the equation

$$k_s = \frac{\sin\gamma}{1 + \cos\gamma - \dfrac{\pi - \gamma}{2}\sin\gamma}\,p \tag{3.6}$$

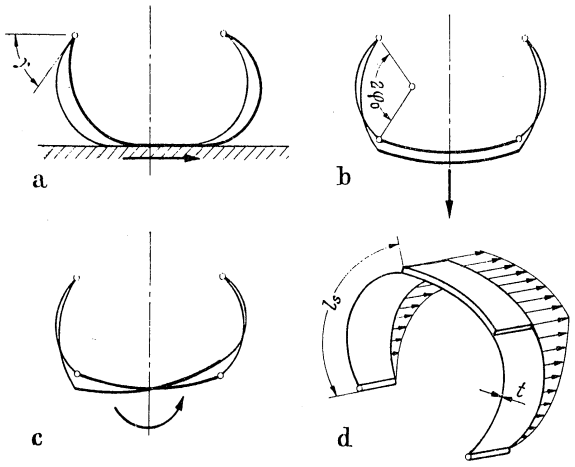

Fig. 10. To derive the elastic stiffnesses of the belt, virtual displacements are given according to the arrows shown: (a) lateral stiffness, k_S; (b) radial stiffness, k_a; (c) torsional stiffness, k_T; (d) tangential stiffness, k_τ.

By analogy, one can show (b), that the radial stiffness k_a is given by

$$k_a = \frac{\cos\varphi_0 + \varphi_0 \sin\varphi_0}{\sin\varphi_0 - \varphi_0 \cos\varphi_0} p \,. \tag{3.7}$$

Similarly, from (c) the torsional stiffness k_T is

$$k_T = k_a \frac{b^2}{4} \,. \tag{3.8}$$

Finally the fore and aft stiffness (d), due to the shear compliance of the radially reinforced side walls, is given by:

$$k_\tau = \frac{G\,t}{l_s} + p \cot\varphi_0 \,. \tag{3.9}$$

4. Equilibrium Equation of the Belted Tire. The equilibrium conditions for the belt are derived from the assumption that the belt has four degrees of freedom: the displacement u in the circumferential direction, the radial displacement v, the transverse deformation w, and the belt torsion φ. These four quantities are functions of the independent variable φ (coordinate in the circumferential direction of the tire) and time t. In the derivation of the equations of motion the nonlinear terms are neglected, but it is still necessary to establish the equilibrium relationships from the deformed belt element. This is so because linear parts of these terms (due to the deformation), have to be included in the equations because of the tension force in the belt T_0 as well as the torsion moment T_M, which is induced by T_0; both of these quantities are present at the beginning of deformation. The theory of the ring has been treated by Federhofer, Volterra, and Rodriguez [4,5,6]. However, the pretension of the belt results in additional terms.

We measure displacements from the midline of the belt, in the form

$$\mathfrak{r} = \mathfrak{r} + e_\varphi u + e_r v + e_b w \,. \tag{4.1}$$

The strain ε of the midline is calculated, using $\partial/\partial\varphi \equiv (\,)'$, as

$$\varepsilon = \frac{|d\bar{\mathfrak{r}}| - |d\mathfrak{r}|}{|d\mathfrak{r}|} = \sqrt{\left(1 + \frac{u' + v}{a}\right)^2 + \left(\frac{w'}{a}\right)^2 + \left(\frac{v' - u}{a}\right)^2} - 1 \,,$$

or after linearization

$$\varepsilon = \frac{u' + v}{a} \,. \tag{4.2}$$

The angle of twist φ of the belt will be taken positive in the sense of a left handed screw as shown in Fig. 11.

If one considers only small displacements u, v, w, and angle φ, the unit vectors $\bar{\mathfrak{t}}$ (in the direction of the belt), $\bar{\bar{\mathfrak{t}}}$ (normal to the direction

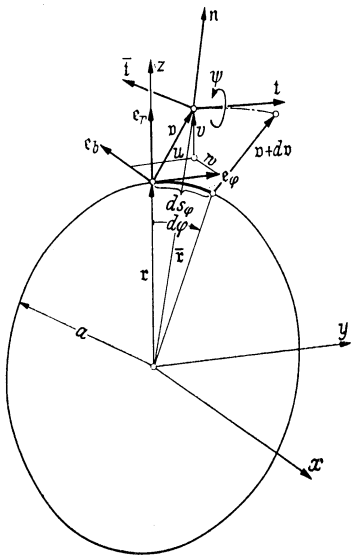

Fig. 11. Sketch of the displacements of the belt.

but in the plane of the belt) and $\bar{n}$ (normal to the belt) are determined from the equations:

$$t = e_\varphi + e_b \frac{w'}{a} + e_r \frac{v' - u}{a}, \qquad \bar{t} = e_\varphi \frac{w}{a} + e_b - e_r \psi, \qquad n = - e_\varphi \frac{v' - u}{a} + e_b \psi + e_r. \quad (4.3)$$

Here $\bar{n}$ is the outer normal and $\bar{t}$, $\bar{\bar{t}}$, and $\bar{n}$ form a right handed system. By the displacement of this orthogonal unit triad an amount ds in the direction of the belt, one can determine a rotation vector $\bar{w}$ by analogy to the Darboux vector of a spatial curve:

$$w = t\left(\frac{w'}{a^2} - \frac{\psi'}{a}\right) + \bar{t}\,\frac{1}{a}\left(1 - \frac{v'' + v}{a}\right) + n\,\frac{1}{a}\left(\frac{w''}{a} + \psi\right). \quad (4.4)$$

The coefficients of the unit vectors represent the torsion and the curvature of the belt.

Now we consider a belt element with the forces and moments acting on it. The force-resultants, and moment-resultants, along the edges are represented separately from the load and moment intensities (Fig. 12). Let ρ be the mass per unit length, $\bar{b}$ the acceleration, and Θ the angular momentum. The mass of the side walls is neglected. Then the equations of equilibrium for the element become

$$\left.\begin{aligned} &\frac{d(T\,t)}{ds_\varphi} + \frac{d(V\,\bar{t})}{ds_\varphi} - \frac{d(Q\,n)}{ds_\varphi} + e_\varphi\,\bar{\tau} + e_b\,\bar{q}_s + e_r\,\bar{q}_a + p\,b^*\,(1+\varepsilon)\,n = \varrho\,\bar{b}, \\ &\frac{d\,(T_M\,t - M_T\,\bar{t})}{ds_\varphi} - \frac{d(M_1\,n)}{ds_\varphi} - \frac{d(M_2\,\bar{t})}{ds_\varphi} + V\,n \\ &+ Q\,\bar{t} + e_\varphi\,\bar{m} + e_r\,\bar{n} + e_b\,\bar{l} = \frac{d\vartheta}{dt} = \frac{d}{dt}\left(-\dot{\psi}\,\frac{b^2 + t^2}{12}\,t + \frac{\dot{w}'}{a}\,\frac{b^2}{12}\,n\right)\varrho, \end{aligned}\right\} \quad (4.5)$$

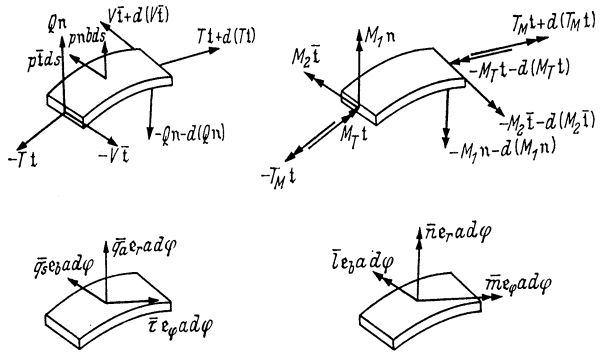

Fig. 12. Forces and moments acting on a tire element for the derivation of the equations of motion of the belt.

where T_M is given by (2.1) and T by (2.2). Using the components of $\overline{w}$ we get:

$$M_T = -G\,I_p\left(\frac{w'}{a^2}-\frac{\psi'}{a}\right), \qquad M_1 = -E\,I_x\left(\frac{w''}{a^2}+\frac{\psi}{a}\right), \qquad M_2 = -E\,I_y\left(\frac{v''+v}{a^2}\right). \tag{4.6}$$

Shear deformations due to the shear forces Q and V are neglected.

By performing the differentiations with respect to the unstrained length of the belt ds_φ, the equations of equilibrium can be written down. Before doing that we wish to define more carefully the load and moment intensities. Let $t(\varphi)$ be the external load in tangential direction, $p(\varphi)$ the external axial load, $q(\varphi)$ the external radial load, h_L the height of the tread, $n(\varphi)$ the external radial moment. The load and moment intensities are now:

$$\left.\begin{aligned} \bar{\tau} &= -k_\tau u + t(\varphi), & \bar{q}_s &= -k_s w + p(\varphi), \\ \bar{q}_a &= -k_a v + q(\varphi), & \bar{m} &= +k_T\psi - h_L\cdot p(\varphi), \\ \bar{n} &= h_L\cdot t(\varphi), & \bar{l} &= -\frac{w'}{a}k_\tau\left(\frac{b}{2}\right)^2 + n(\varphi). \end{aligned}\right\} \tag{4.7}$$

Finally the equations of equilibrium become:

$$
\left.
\begin{aligned}
&E\,F\frac{u''+v'}{a^2}-\frac{1}{a}Q-k_\tau\,u+t_{(\varphi)}=\ddot{u}\varrho\,,\\
&T_0\frac{w''}{a^2}+\frac{1}{a}V'-k_s\,w+p(\varphi)+p\,b^*\psi=\ddot{w}\,\varrho\,,\\
&T_0\frac{v''+v}{a^2}-E\,F\frac{u'+v}{a^2}-\frac{1}{a}Q'-k_a\,v+q(\varphi)=\ddot{v}\,\varrho\,,\\
&\frac{d\tan\beta}{2\,a}\left(T_0\frac{v'-u}{a}+E\,F\frac{u''+v'}{a}\right)+\frac{G\,I_p}{a}\left(\frac{w''}{a^2}-\frac{\psi''}{a}\right)\\
&\quad+\frac{E\,I_x}{a}\left(\frac{w''}{a^2}+\frac{\psi}{a}\right)+k_T\psi-h_L\,p(\varphi)=-\ddot{\psi}\,\varrho\,\frac{b^2+t^2}{12}\,,\\
&\frac{d\tan\beta}{2\,a}\,T_0\frac{w''}{a}-E\,I_y\frac{v'''+v'}{a^3}+Q+h_L\,t(\varphi)=0\,,\\
&\frac{d\tan\beta}{2\,a}\left[T_0\left(\frac{v''-u}{a}-1\right)-E\,F\frac{u'+v}{a}\right]-\frac{G\,I_p}{a}\left(\frac{w'}{a^2}-\frac{\psi'}{a}\right)\\
&\quad+\frac{E\,I_x}{a}\left(\frac{w'''}{a^2}+\frac{\psi'}{a}\right)+V-\frac{w'}{a}k_\tau\left(\frac{b}{2}\right)^2+n(\varphi)=\frac{\ddot{w}'}{a}\,\varrho\,\frac{b^2}{12}\,.
\end{aligned}
\right\}
\tag{4.8}
$$

These are six equations in the six unknowns u,v,w,φ,V,Q. The inertia terms are given here for the tire which is not rotating. One obtains the inertia terms for the rotating tire by considering that the tire elements are equivalent with respect to the circumferential coordinate and that they pass a deformation field which varies with time with the angular speed Ω. This description, named after Euler, requires use of substantial derivatives.

Let $\bar{v} = \bar{v}(\varphi,t)$ be the field of deformations with respect to an observer at rest. Let the center 0 be stationary (Fig. 11) which is the situation on the road wheel. Then the absolute velocity is given by:

$$
\frac{D\bar{r}}{Dt}=\frac{Dr}{Dt}+\frac{D\mathfrak{v}}{Dt}=e_\varphi\,a\,\Omega+\frac{D\mathfrak{v}}{Dt}\,.
$$

The substantial derivative D/Dt follows from:

$$
\frac{D\mathfrak{v}}{Dt}=\frac{\partial\mathfrak{v}}{\partial t}+\frac{\partial\mathfrak{v}}{\partial s_\varphi}\frac{ds_\varphi}{dt}=\dot{\mathfrak{v}}+\Omega\,\mathfrak{v}'\,.
$$

And therefore

$$
\frac{D\bar{r}}{Dt}=e_\varphi\,\Omega\,a+\dot{\mathfrak{v}}+\Omega\,\mathfrak{v}'\,.
$$

We then obtain the acceleration as the substantial derivative of the velocity

$$
\frac{D^2\bar{r}}{Dt^2}=\mathfrak{b}=-e_r\,a\,\Omega^2+\ddot{\mathfrak{v}}+2\,\Omega\,\dot{\mathfrak{v}}'+\Omega^2\mathfrak{v}''\,,
$$

and substituting the component of the displacement vector

$$\frac{D\bar{\mathfrak{r}}}{Dt} = e_\varphi [a\,\Omega + \dot{u} + \Omega\,(u' + v)] + e_b\,(\dot{w} + \Omega\,w') + e_r\,[\dot{v} + \Omega(v' - u)\,, \tag{4.9}$$

$$\frac{D^2\bar{\mathfrak{r}}}{Dt^2} = e_\varphi\,[\ddot{u} + 2\,\Omega\,(\dot{u}' + \dot{v}) + \Omega^2\,(u'' + 2\,v' - u)] + e_b\,(\ddot{w} + 2\,\Omega\,\dot{w}' + \Omega^2 w'')$$
$$+ e_r\,[\ddot{v} + 2\,\Omega\,(\dot{v}' - \dot{u}) + \Omega^2\,(v'' - 2\,u' - v - a)]\,. \tag{4.10}$$

Note that the rotation vector $\bar{w}$ represents the rotations of the triad along ds_φ. This might be used to determine the absolute angular momentum of the belt element. Therefore there arises an additional term due to the rotation

$$\mathfrak{w}\,\dot{s}_\varphi = \mathfrak{w}\,a\,\Omega\,.$$

Hence the angular momentum vector becomes

$$\vartheta = \left[-\dot{\psi} + \Omega\left(\frac{w'}{a} - \psi'\right)\right]\varrho\,\frac{b^2 + t^2}{12}\,\mathfrak{t} + \left[\frac{\dot{w}'}{a} + \Omega\left(\frac{w''}{a} + \psi\right)\right]\varrho\,\frac{b^2}{12}\,\mathfrak{n}\,,$$

and after linearization

$$\vartheta = e_\varphi\left[-\dot{\psi} + \Omega\left(\frac{w'}{a} - \psi'\right)\right]\varrho\,\frac{b^2 + t^2}{12} + e_r\left[\frac{\dot{w}'}{a} + \Omega\left(\frac{w''}{a} + \psi\right)\right]\varrho\,\frac{b^2}{12}\,.$$

Hence

$$\frac{D\vartheta}{Dt} = \frac{\partial\vartheta}{\partial t} + \frac{\partial\vartheta}{\partial\varphi}\,\Omega\,,$$

and the substantial rate of change of the absolute angular momentum is

$$\frac{D\vartheta}{Dt} = e_\varphi\left[(-\ddot{\psi} - 2\,\dot{\psi}'\,\Omega - \psi''\,\Omega^2)\,\varrho\,\frac{b^2 + t^2}{12} + \left(\frac{\dot{w}'}{a} + \frac{w''}{a}\,\Omega\right)\Omega\,\varrho\,\frac{2\,b^2 + t^2}{12} + \psi\,\Omega^2\,\varrho\,\frac{b^2}{12}\right]$$
$$+ e_r\left[\left(\frac{\ddot{w}'}{a} + 2\,\frac{\dot{w}''}{a}\,\Omega + \frac{w'''}{a}\,\Omega^2\right)\varrho\,\frac{b^2}{12} + (\dot{\psi} + \psi'\,\Omega)\,\Omega\,\varrho\,\frac{2\,b^2 + t^2}{12} - \frac{w'}{a}\,\Omega^2\varrho\,\frac{b^2 + t^2}{12}\right]. \tag{4.11}$$

5. Illustrations of the Theory by Static Axial Deflections, Radial Vibrations and the Formation of Stationary Waves at High Rolling Speed. During rolling the steering properties are heavily influenced by the axial deflections due to the effect of side forces. As a simple example consider the static axial deflection caused by a external load $p(\varphi)$ acting from the side in the direction $\bar{e}_b$. In the equations of equilibrium we consider only the unknowns, w, φ, and v and arrive at the three equations

$$\left.\begin{aligned} &T_0\frac{w''}{a^2}+\frac{1}{a}V'-k_s w+p(\varphi)+p\,b^*\psi=0\,,\\ &\frac{G\,I_p}{a}\left(\frac{w''}{a^2}-\frac{\psi''}{a}\right)+\frac{E\,I_x}{a}\left(\frac{w''}{a^2}+\frac{\psi}{a}\right)+k_T\psi-h_L\,p(\varphi)=0\,,\\ &-\frac{G\,I_p}{a}\left(\frac{w'}{a^2}-\frac{\psi'}{a}\right)+\frac{E\,I_x}{a}\left(\frac{w'''}{a^2}+\frac{\psi'}{a}\right)+V-\frac{w'}{a}k_\tau\left(\frac{b}{2}\right)^2=0\,. \end{aligned}\right\} \tag{5.1}$$

Let p = p_0 be the transverse load for $-\varphi^* \leq \varphi \leq +\varphi^*$ and p = 0 elsewhere

$$p(\varphi)=p_0\frac{\varphi^*}{\pi}\left(1+2\sum_{\nu=1}^{\infty}\frac{\sin\nu\varphi^*}{\nu\varphi^*}\cos\nu\varphi\right).$$

We eliminate from (5.1) the axial force v and neglect the small terms $h_L p(\varphi)$ and $\frac{w'}{a}\,k_\tau(b/2)^2$, thus obtaining:

$$\left.\begin{aligned} &-\frac{E\,I_x}{a^2}w''''+\left(T_0+\frac{G\,I_p}{a^2}\right)w''-k_s\,a^2\,w=-p\,b^*\,a^2\psi+\left(\frac{E\,I_x}{a}+\frac{G\,I_p}{a}\right)\psi''-a^2\,p(\varphi)\,,\\ &\frac{G\,I_p}{a^2}\psi''-\left(\frac{E\,I_x}{a}+k_\tau a\right)\psi=\left(\frac{G\,I_p}{a^2}+\frac{E\,I_x}{a^2}\right)w''\,. \end{aligned}\right\} \tag{5.2}$$

The second equation is homogeneous. A Fourier expansion

$$w(\varphi)=\sum_{\nu=0}^{\infty}w_\nu\cos\nu\varphi\,,\qquad \psi(\varphi)=\sum_{\nu=0}^{\infty}\psi_\nu\cos\nu\varphi \tag{5.3}$$

yields

$$\psi_\nu=\frac{\left(\frac{E\,I_x}{a^2}+\frac{G\,I_p}{a^2}\right)\nu^2 w_\nu}{\frac{E\,I_x}{a^2}+k_T a+\frac{G\,I_p}{a}\nu^2}. \tag{5.4}$$

and this substituted into (5.2) leads to:

$$w_\nu=\frac{a^2 p_\nu}{\frac{E\,I_x}{a^2}\nu^4+\left(T_0+\frac{G\,I_p}{a^2}\right)\nu^2+k_s a^2-\frac{\left[\nu^2\left(\frac{G\,I_p}{a}+\frac{E\,I_x}{a}\right)+p\,b^*\,a^2\right]\nu^2\left(\frac{G\,I_p}{a}+\frac{E\,I_x}{a}\right)}{G\,I_p\,\nu^2+EI_x+a^2\,k_T}}. \tag{5.5}$$

As an example we calculate the axial deflection under the load p_0 = 1.0 kp/cm with φ^* = 11° for a belted tire with the following characteristics:

a = 30 cm	b^* = 10 cm	p = 1.5 atü
γ = 60°	β_G=0°	G = 50 kp/cm
I_p = 84 cm⁴	β = 18.5°	EI_x = 0.56 · 10⁶ kp/cm²
T_0 = 400 kp	k_s = 2.2 kp/cm²	k_T = 75 kpcm/cm.

The substitution of these numerical values into (5.4), (5.5) and graphical superposition of the different waves yields the deformation shown in Fig. 13. These calculated deflections compare very well with those measured by Hinton and Frank and also by Borgmann [1,2,3]. Taking into account the

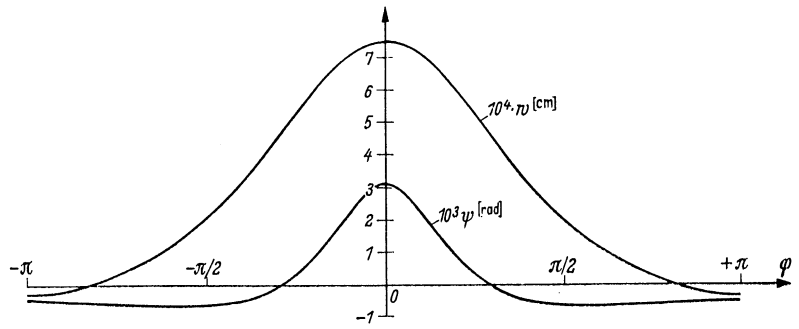

Fig. 13. Static axial deflections of the belt under a lateral load.

moment intensity n and its first derivative dn/ds, one might calculate from (5.5) the distortion of the belt due to radial bending, the flattening and the rotation of the moments of the pretension.

Another example is the vibration of the belt in the plane of the wheel. The only unknowns now are the displacements u and v. We get the two equations:

$$\left.\begin{aligned} \frac{EF}{a^2}(u'' + v') - \frac{EI_y}{a^4}(v''' + v') &= \varrho\,\ddot{u} + k_\tau u, \\ \frac{T_0}{a^2}(v'' + v) - \frac{EF}{a}(u' + v) - \frac{EI_y}{a^4}(v'''' + v'') + q &= \varrho\,\ddot{v} + k_a v. \end{aligned}\right\} \tag{5.6}$$

A sinusoidally varying load q, may act in the area of contact in radial direction. We determine the natural frequencies $\omega_e = \sqrt{\lambda/\varrho}$ by the assumption

$$u = A \sin \omega_e t \sin n\varphi, \qquad v = B \sin \omega_e t \cos n\varphi, \tag{5.7}$$

where n is the wave number at the circumference and is obtained from the determinant

$$\begin{vmatrix} \frac{EF}{a^2}n^2 + k_\tau - \varrho\,\omega_e^2 & \frac{EF}{a^2}n + \frac{EI_y}{a^4}(n^2-1)n \\ \frac{EF}{a^2}n & \frac{T_0}{a^2}(n^2-1) + \frac{EF}{a^2} + \frac{EI_y}{a^4}(n^2-1)n^2 + k_a - \varrho\,\omega_e^2 \end{vmatrix} = 0. \tag{5.8}$$

For the same numerical values as above the result for the different wave forms (n = 1,...,5) is shown in Table 1 ($EF = EI_x/i_x = 6.72 \times 10^4$ kp and $EI_y = .14 \times 10^4$ kp/cm^2, density $\rho = 4.45 \times 10^{-5}$ kpsec^2/cm, $k_\tau = 3.3$ kp/cm^2, and $k_a = 26$ kp/cm^2). The frequency ω_1 corresponds to a longitudinal vibration, while ω_2 corresponds to an axial vibration. If $\omega \neq \omega_e$ (Fig. 14) we use the following linear equations in order to determine the amplitudes A and B:

$$
\left.
\begin{aligned}
-\frac{E\,F}{a^2}(A\,n^2 + B\,n) - \frac{E\,I_y}{a^4}(n^2-1)\,n\,B &= -\varrho\,\omega^2 A + k_t\,A,\\
\frac{T_0}{a^2}(1-n^2)\,B - \frac{E\,F}{a^2}(A\,n + B) - \frac{E\,I_y}{a^4}(n^2-1)\,n^2\,B + q_n &= -\varrho\,\omega^2\,B + k_a\,B,
\end{aligned}
\right\} \tag{5.9}
$$

TABLE 1

n	1	2	3	4	5
ω_1	1920 sec^{-1}	2930 sec^{-1}	4120 sec^{-1}	5350 sec^{-1}	7010 sec^{-1}
ω_2	549 sec^{-1}	695 sec^{-1}	782 sec^{-1}	850 sec^{-1}	914 sec^{-1}
$\omega_2/2\pi$	87.5 Hz	110.7 Hz	124 Hz	124 Hz	145 Hz

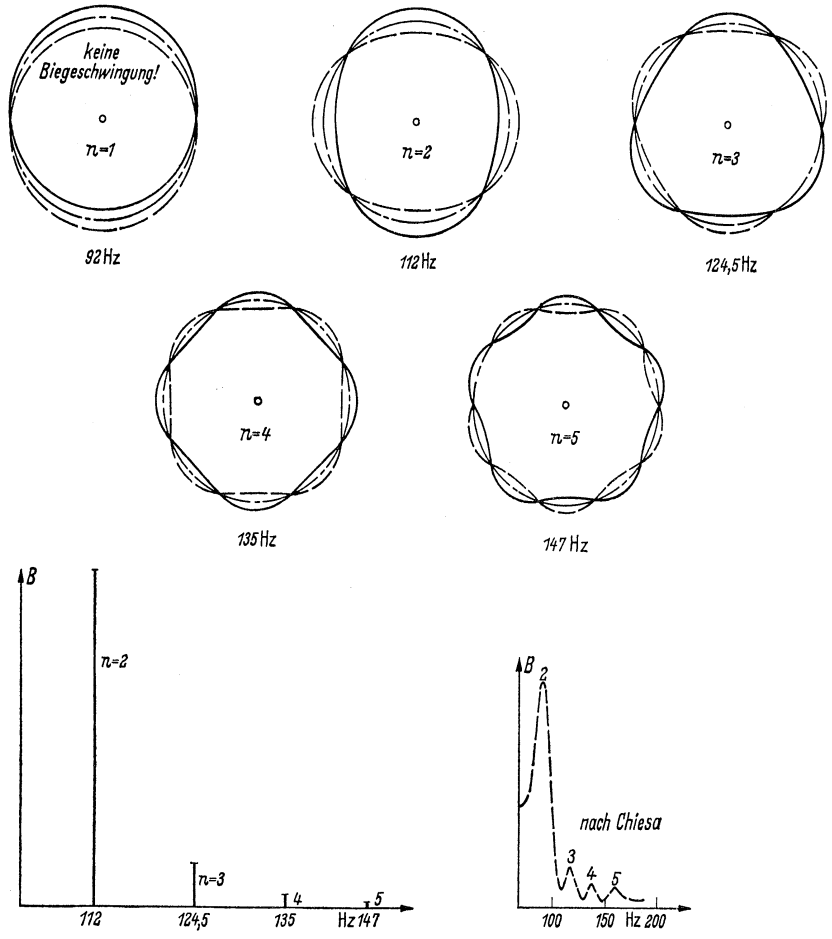

Fig. 14. Radial natural vibrations and resonance of the belt tire.

In the case of resonance the amplitudes can only be determined if one takes the energy dissipation into account. The dissipation is a consequence of the hysteresis in the rubber. We therefore assume that the energy loss is proportional to the stored elastic energy when the displacements are a maximum.

$$A_{Diss.} = (0{,}2 \text{ bis } 0{,}3)\, A_{El.} = A_{Err.}\,, \tag{5.10}$$

which must be replaced by the excitation. Let us now consider the transverse waves. We find the damping energy by comparison with the elastic bending energy at t = T/4 (belt with foundation)

$$A_{El.,\text{Bend.}} = \frac{1}{2} \int_{\varphi=0}^{2\pi} \frac{M_2^2}{E\, I_y}\, a\, d\varphi\,, \qquad \text{becomes} \qquad A_{El.,\text{Bend.}} = \frac{\pi}{2} \frac{E\, I_y}{a^2} \sum_{n=2}^{\infty} (n^2 - 1)^2\, B\,,$$

or if only the resonance applitude is taken into account:

$$A_{El.,\text{Bend.}} = \frac{\pi}{2} \frac{E\, I_y}{a^2} (n^2 - 1)\, B_n\,. \tag{5.11}$$

In the state of resonance v and q make a phase angle of 90° and therefore

$$v_{res.} = -\cos \omega_e t \,(\sum_{n=1}^{\infty} B_n \cos n\varphi)$$

or

$$A_{Err.} = \int_{-\varphi^*}^{+\varphi^*} [\int_{t=0}^{t=T} q\, v_{res.}\, dt]\, a\, d\varphi = 2\,\varphi^*\, a\pi\, (\sum_{n=1}^{\infty} B_n q_n)$$

$$A_{Err.} \doteq 2\,\varphi^*\, a\pi\, B_n\, q_n\,. \tag{5.12}$$

For the values q_n = 1.0 kp/cm and (5.10) we obtain the amplitude ratios shown in Fig. 14 (independent of the ratio of dissipated energy and deformation energy and independent of the point of disturbance on the circumference). These amplitude ratios and natural frequencies coincide with those measured by Chiesa, Oberto, and Tamburini [10]. The resonance amplitude for n = 1 may be determined from the hysteresis (loss) energy during the shear deformation of the side walls.

In the same way the natural frequencies of axial vibrations are determined. From the assumption

$$w = A \sin \omega_e t \cos n\varphi \quad \text{and} \quad \psi = B \sin \omega_e t \cos n\varphi$$

we get the determinant for the eigenvalues

$$\begin{vmatrix} \frac{T_0}{a^2}n^2 + \frac{G\,I_p}{a^4}n^2 + \frac{E\,I_x}{a^4}n^4 + \frac{k_\tau}{a^2}\left(\frac{b}{2}\right)^2 n^2 + k_s - \varrho\,\omega_e^2\left(1 + \frac{b^2}{12a^2}n^2\right) & \frac{G\,I_p}{a^3}n^2 + \frac{E\,I_x}{a^3}n^2 + p\,b^* \\ \frac{G\,I_p}{a^3}n^2 + \frac{E\,I_x}{a^3}n^2 & \frac{G\,I_p}{a^2}n^2 + \frac{E\,I_x}{a^2} + k_T - \varrho\,\omega_e^2\frac{b^2+t^2}{12} \end{vmatrix} = 0. \qquad (5.13)$$

As a third example we investigate the formation of stationary waves at high rolling speeds, and for this consider the situation on a road wheel (Fig. 15). The stationary wave affects the belt and the side walls and it decays along the circumference. As a simplification we neglect the deflection u in the direction of the circumference and also the bending effect (EI_y) of the belt. Then using (4.8) and (4.10) the equations of motion for v become:

$$-\frac{T_0}{a^2}(v'' + v) + \frac{E\,F}{a^2}v + \Omega^2\varrho\,(v'' - v - a) + k_a\,v = 0$$

or

$$-\left(\frac{T_0}{a^2} - \varrho\,\Omega^2\right)v'' + \left(k_a + \frac{E\,F}{a^2} - \varrho\,\Omega^2 - \frac{T_0}{a^2}\right)v = \varrho\,a\,\Omega^2. \qquad (5.14)$$

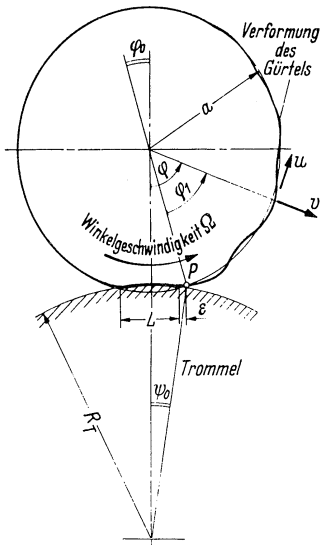

Fig. 15. Stationary wave on the road wheel.

The solution to this differential equation is either a decaying exponential function for $\Omega < \Omega_1$ or for $\Omega_1 < \Omega < \Omega_2$ it is an undamped vibration. The two critical angular velocities are determined from

$$\Omega_1 = \sqrt{\frac{T_0}{\varrho\, a^2}} \qquad \text{and} \qquad \Omega_2 = \sqrt{\frac{k_a + \frac{E\,F}{a^2} - \frac{T_0}{a^2}}{\varrho}}. \tag{5.15}$$

For a Michelin belted tire of 135-13, size, described in Section 6, Ω_1 = 126 sec^{-1} (which corresponds 124 km/h) and Ω_2 = 2350 sec^{-1} (2300 km/h). The critical angular velocity Ω_2 is meaningless, since the belt breaks between 200 and 250 km/h by cracking from the edge.

The introduction of a damping factor into the equations of motion (5.14) causes the solution for the stationary wave to decay along the circumference. The belt with a base or foundation (three-layer belt) has only little damping, but the two-layer belt utilizes the damping in the intervening rubber so that we have, analogous to (2.2)

$$T = T_0 + E\,F\,\varepsilon + k_d\,\dot{\varepsilon}\,, \tag{5.16}$$

We use for the hysteresis in rubber an equivalent damping factor

$$k_d = \frac{4\,d}{\pi\,A\,\omega} = \frac{4\,E\,F}{10\,\pi\,\omega}, \tag{5.17}$$

where the quantities d,A, and B are given in Fig. 16 and d/B has been set equal to 1/10. The frequency has been denoted by ω and is for hysteresis calculations independent of damping. If one takes the substantial derivative of the strain

$$\frac{D\varepsilon}{Dt} = \frac{\partial\varepsilon}{\partial t} + \frac{\partial\varepsilon}{\partial\varphi}\,\Omega = \frac{v'}{a}\,\Omega \tag{5.18}$$

$\partial\varepsilon/\partial t$ = 0 since we have a stationary state, then the equations of motion become

$$-\left(\frac{T_0}{a^2} - \varrho\,\Omega^2\right)v'' + \frac{k_d}{a}\,v' + \left(k_a + \frac{E\,F}{a^2} - \varrho\,\Omega^2 - \frac{T_0}{a^2}\right)v = \varrho\,a\,\Omega^2. \tag{5.19}$$

An approximate solution for $\Omega_1 < \Omega$ is

$$v = A\,e^{-\lambda\varphi_1}\sin\omega\varphi_1 \tag{5.20}$$

with the constants

$$\lambda = \frac{1}{2}\,\frac{k_d}{a\,\varrho\,\Omega^2 - \frac{T_0}{a}} \qquad \text{and} \qquad \omega = \sqrt{\frac{k_a + E\,F - \varrho\,\Omega^2 - \frac{T_0}{a^2}}{\varrho\,\Omega^2 - \frac{T_0}{a^2}}}. \tag{5.21}$$

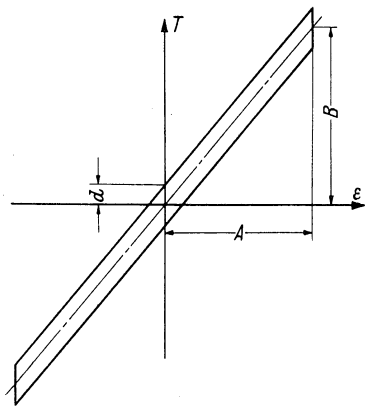

Fig. 16. Assumed hysteresis of a belt which is not attached to a tire.

The ratio of two consecutive amplitudes is

$$D = \frac{A_{n+1}}{A_n} = e^{-\pi \lambda/\omega}. \tag{5.22}$$

These effects on the belt assume a maximum in the first wave behind the area of contact. In order to determine the extreme amplitude A_{max} we might fix as a good approximation for the initial conditions at point P (Fig. 15)

$$v_p = 0 \quad \text{and} \quad v_p' \doteq \left(1 + \frac{a}{R_T}\right)\left(\frac{L}{2} + \varepsilon\right). \tag{5.23}$$

Hence we get

$$A_{max} = \frac{v_p'}{\omega} \cdot \left(1 - \frac{D}{2}\right) = \left(1 + \frac{a}{R_T}\right)\left(\frac{L}{2} + \varepsilon\right)\frac{1}{\omega}\left(1 - \frac{D}{2}\right). \tag{5.24}$$

The additional belt force ΔT due to the formation of the wave is then

$$\Delta T = E F \frac{A_{max}}{a}. \tag{5.25}$$

6. Measurements of Radial and Axial Vibrations of a Michelin Belted Tire of Size 135-13 and Comparison With the Theory. The theory of the belted tire described in the previous sections has been compared with measurements[2] of radial and axial vibrations on a Michelin X tire 135-13 of German manufacture. Although radial vibrations have already been investigated by Chisea, Oberto, and Tamburini [10], the axial vibrations which are essential for the driving

[2]The measurements were performed within the above-mentioned Diplomarbeit.

properties have not yet been determined. The main concept was to calculate back certain characteristic parameters from the measured frequencies and to compare them with the terms developed from the theory of the belted tire. The different stiffness of the belted tire and elastic dependence upon the belt pretension were to be determined.

The tire was mounted on the rim and attached to a steel frame. By loosening a nut the tire could be rotated about arbitrary angles. For measurements of radial vibrations the exciter was mounted on a channel, while for measurements of axial vibrations it hung on a structure (Figs. 17 and 18). In the middle of the tire on Fig. 17 one may recognize the accelerometer,[3] which was cemented onto the tire. For axial vibrations it was attached to a piece of wood which again was cemented to the tread of the tire. During the measurements of the amplitudes the point of excitation was changed by rotating the tire in steps of 15°. Having determined the natural frequencies (resonant points) by measuring the acceleration at a point opposite to the exciter one can measure the amplitudes along the circumference. It was assumed that the tire was completely axisymmetric.

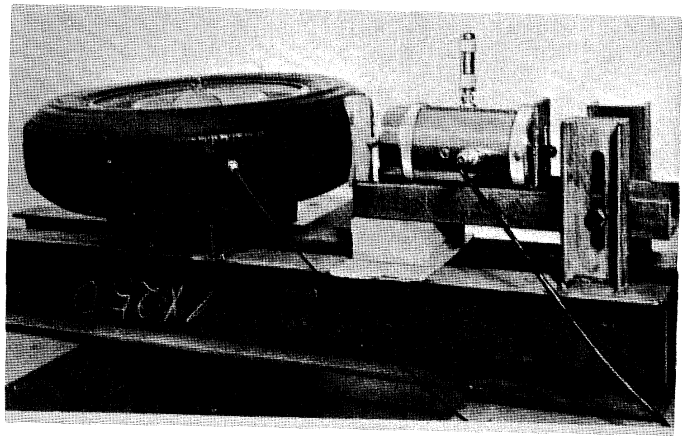

Fig. 17. Experimental equipment for measurements of radial vibrations.

[3]Equipment used for measurements: On the side of the exciter a sinusoidal wave generator with attached force amplifier and electromagnetic exciter. On the measuring side a piezoelectro transducer with amplifier and integration network. In order to determine the points of resonance the phase was observed by a dual trace oscillator.

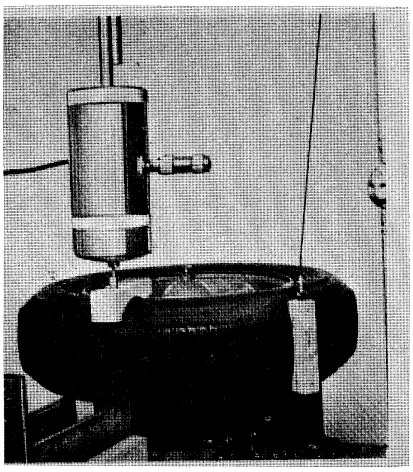

Fig. 18. Experimental equipment for measurements of axial vibrations.

Measurements have been performed several times and average natural frequencies have been determined. The accuracy was 2-3% of the scale value. Figures 19 and 20 show the wave forms for radial and axial vibrations. In addition, frequency-amplitude diagrams have been determined for the point opposite to the exciter.

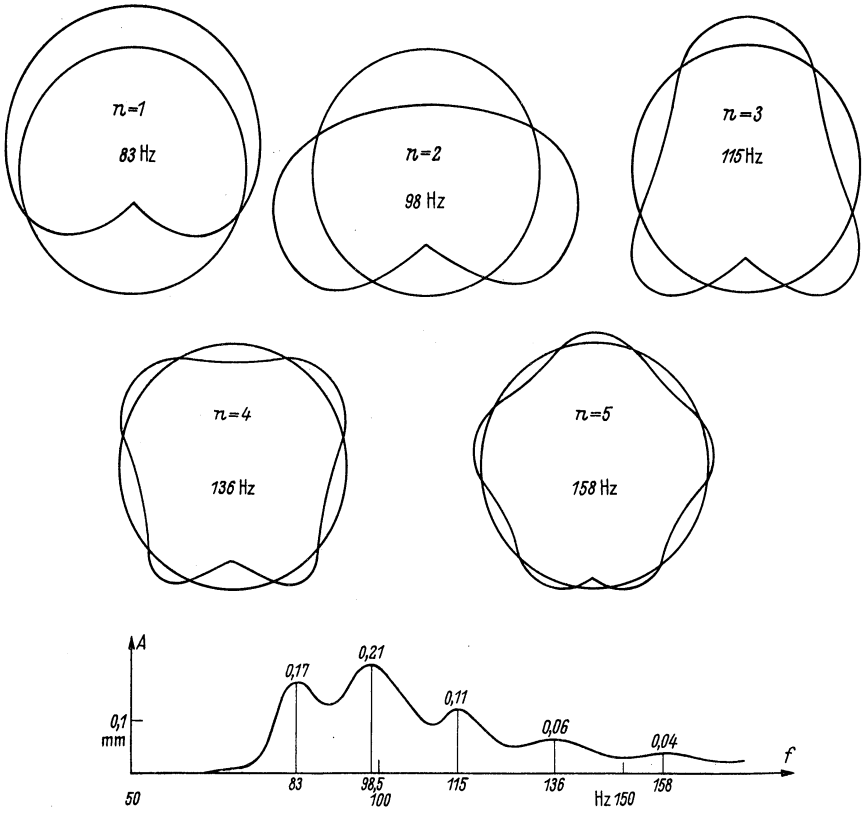

Fig. 19. Wave forms and resonance curve for radial vibration.

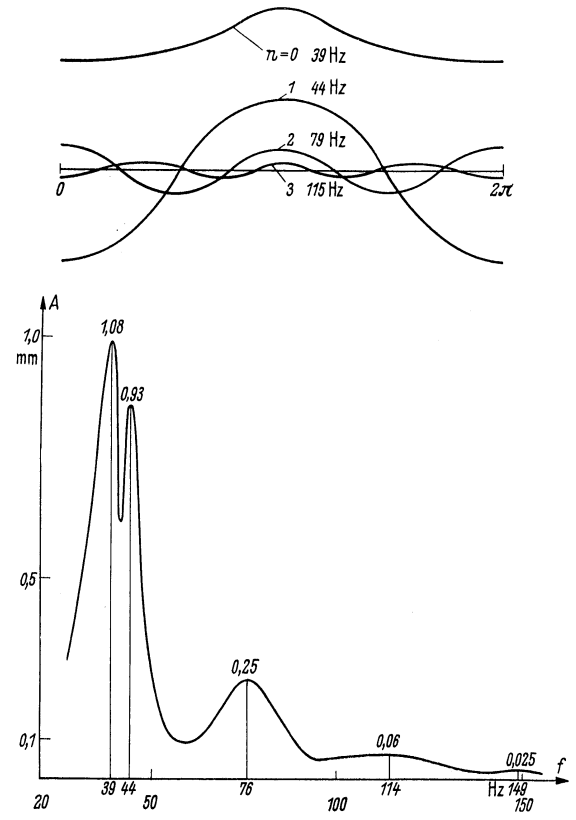

Fig. 20. Wave forms and resonance curve for axial vibration.

After measurements of vibration the available characteristic tire data have been obtained in a relatively rough way. Then the tire was cut and the width of the belt, ply thickness, thickness of the side wall, and so on have been determined from a section. Elastic constants have not been measured. The values gotten in this way are given in Fig. 21. In order to determine the characteristics of the belted tire from the measured natural frequencies and the approximate belted tire theory one needs considerable mathematical work. Although it is relatively easy to get the frequencies from the characteristic data (one has only to use the eigenvalue equations), it is much more difficult to calculate the characteristic quantities back from given frequencies, since the equations to be solved are nonlinear. Some of the characteristic data, however, can be estimated simply. For example one can calculate the stiffness k_a by using the natural frequency of a rigid ring having the mass of the belt and then determining the equation for this frequency by Rayleigh's method. For a rigid ring on an elastic foundation, one obtains

$$k_r + k_a = 2\,\varrho\,\omega_1^2. \tag{6.1}$$

With the mass of the belt measured to $\rho = 1.59 \times 10^{-5}$ kpcm^{-2} sec^2, the measured frequency $\omega_1 = 516$ sec^{-1} and the calculated $k_T = 1.3$ kp cm^{-2} Eq. (6.1) yields $k_a = 7.16$ kp cm^{-2}.

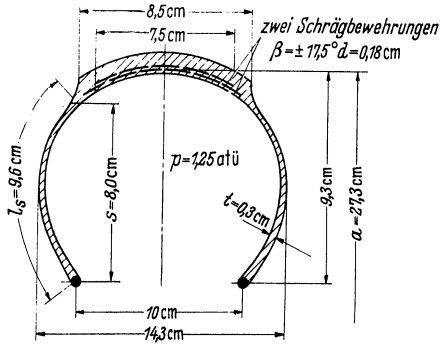

Fig. 21. Dimensions of the belted tire used in these experiments.

The determinant for the frequency of the radial vibration n = 1 of the elastic ring is

$$\begin{vmatrix} \frac{EF}{a^2} + k_r - \varrho\,\omega_1^2 & \frac{EF}{a^2} \\ \frac{EF}{a^2} & \frac{EF}{a^2} + k_a - \varrho\,\omega_1^2 \end{vmatrix} = 0\,,$$

or after multiplication

$$\frac{EF}{a^2}(k_r + k_a - 2\,\varrho\,\omega_1^2) + (k_a - \varrho\,\omega_1^2)(k_r - \varrho\,\omega_1^2) = 0\,. \tag{6.2}$$

Different values of the stiffness k_a in (6.2) leads to EF and the curve shown in Fig. 22. Since EF must be positive, only values greater than 7.16 are possible for k_a. In the same way the transverse stiffness k_S can be obtained assuming that the rigid ring undergoes parallel vibrations out of its plane. One has the relationship

$$k = \varrho\,\bar{\omega}_0^2\,. \tag{6.3}$$

With the measured natural frequency $\omega_1 = 245$ sec^{-1} we obtain $k_S = .995$ kp/cm^2. Finally one can also find the torsional stiffness for one form of vibration, where a rigid ring vibrates about one of its diameters. One has the equation

$$k_s + \frac{1}{a^2}k_T = \varrho\,\bar{\omega}_2^2\,. \tag{6.4}$$

With the measured $\omega_1 = 276$ sec^{-1} and the $k_S = .995$ calculated above we get $k_T = 162$ kp cm/cm rad. If k_S varies one finds the curve shown in Fig. 22.

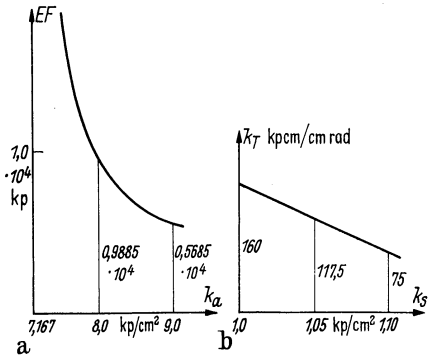

Fig. 22. Calculation of characteristic quantities.
(a) Elasticity of the belt vs. radial stiffness.
(b) Torsional stiffness vs. lateral stiffness.

But now the possibilities of simple calculations using stiffness data are exploited. Important quantities like the pretension of the belt, its circumferencial stiffness and the bending stiffness for radial bending cannot be determined directly. For these calculations a computer program was set up which could solve four nonlinear equations with four unknowns by an iteration technique based on Newton's method and generalized to four dimensions. The radius of convergence in this case has been calculated by trial and error and appear to be extremely small. The calculations were handled as follows: one started off with an assumed set of characteristic parameters and the resulting frequencies of radial vibrations ω_1 to ω_5 were determined by means of the eigenvalue Eq. (5.8). The unknown quantities (EF), T_o, (EI_y), and k_a were temporarily assumed in a rational way. The solution to the nonlinear equations were programmed such, that

$$\omega_{n,\text{calculated}} - \omega_{n,\text{measured}} = 0 \ .$$

The four equations were solved iteratively by a proper variation of the above-mentioned four quantities. Because of the small radius of convergence this could not be accomplished in only one step. Therefore the interval of the difference of the ω-values was divided into one hundred parts. Then the equations, beginning with the calculated values, were evaluated in 100 steps, up to the measured values. Figure 23a-d shows this procedure of calculation. The scattered distributions are due to errors resulting from the discrete-step method and also due to the minor influence of (EI_y). The procedure broke down after 83 steps and no longer converged. A complete calculation of the characteristic data from the measured frequencies was therefore not possible. The remaining error, however, is very small, namely less than

2.7% per frequency. The characteristic data achieved at this limit are already in very good agreement with the measured natural frequencies:

$$f_2 = 100.5 \text{ Hz}, \quad f_3 = 115.6 \text{ Hz}, \quad f_4 = 134.5 \text{ Hz}, \quad f_5 = 154.2 \text{ Hz}.$$

It is interesting that the quantity k_a may fall below the limit 7.16 kp/cm^2, which can only be explained by the fact that k_a has less influence on higher wave forms than for n = 1.

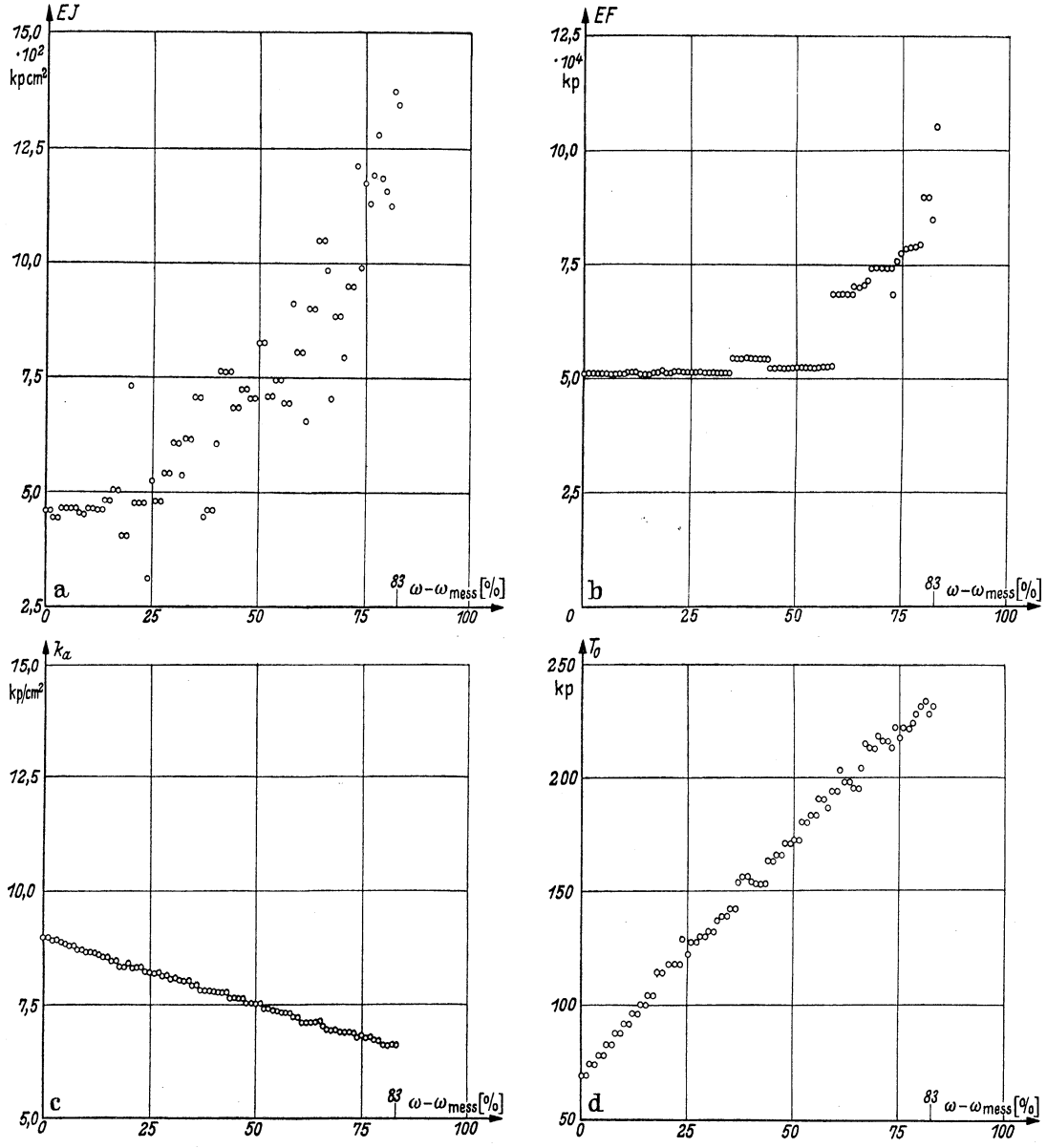

Fig. 23. Solutions to the nonlinear system of equations for four unknown characteristic quantities dependent upon given frequencies. (a) Bending stiffness of the belt about the y-axis; (b) Elasticity of the belt; (c) Radial stiffness; (d) Belt tension.

Until now only three characteristic quantities of the tire (radius a, mass ρ, and the more accurately calculated quantity k_T) have been used. The other four stiffness factors have been found with the aid of the measured natural frequencies and the eigenvalue equations. Now, in contrast, we wish to calculate the tire parameters from the dimensions given in Fig. 21 and the theoretical considerations in Sections 2 and 3. One finds with $s/\ell_s = 0.84$ the value $2\varphi_o = 115°$, from this with (3.8) $k_a = 7.63$ kp/cm^2. From (3.6) and the approximate $\gamma = 45°$ we get $k_s = 1.01$ kp/cm^2. Using (3.8), then $k_T = 107$ kp cm/cm rad. With d = .18 cm, $\nu_G = .5$ and tan $\beta = 0.315$, we obtain from (2.19 the value $\lambda = .75$ and from (2.27) the reduced width of the belt b* = 5.6 cm. From (2.7), using the reduced belt width and $E_G = 150$ kp/cm^2 the circumferential stiffness (EF) = 6.0×10^4 kp, and from (2.29) the bending stiffness (EI_x) = 1.5×10^5 kp cm^2. Then we get from (2.30) the bending stiffness in the normal direction (EI_y) = 706 kp cm^2. From (3.5) the belt tension becomes $T_o = 195$ kp. Finally we calculate from (2.31) the torsional stiffness (GI_p) = 3230 kp cm^2. For the calculation of the eigenvalues from (5.8) and (5.13) all necessary numerical values are arranged once again in Table 2:

TABLE 2

a	= 27.3 cm	T_o	= 195 kp
b	= 7.5 cm	(E F)	= $6.0 \cdot 10^4$ kp
p	= 1.25 kp/cm^2	($E I_x$)	= $1.5 \cdot 10^5$ kp cm^2
k_T	= 1.30 kp/cm^2	($E I_y$)	= $7.06 \cdot 10^2$ kp cm^2
k_a	= 7.63 kp/cm^2	($G I_p$)	= $3.23 \cdot 10^3$ kp cm^2
k_T	= 107 kp/cm/rad	ρ	= $1.59 \cdot 10^{-5}$ kp sec^2/cm^2
k_s	= 1.01 kp/cm^2		

With these values the natural frequencies f_n were calculated (Table 3). The calculated and measured frequencies agree with acceptable accuracy. For the higher axial frequency $\bar{f}_3$ the effect of the torsion of the belt seems to be greater than expressed in the Eqs. (3.8) and (2.31). For $\bar{f}_5$, however, one can conclude from the small resonance amplitude (Fig. 20) that large material damping is present.

TABLE 3

	n = 1	n = 2	n = 3	n = 4	n = 5
Radial vibration					
calculated f, Hz	83.7	105.5	119.0	134.0	150.0
measured f, Hz	83	98.5	115	136	158
	n = 0	**n = 1**	**n = 2**	**n = 3**	**n = 4**
Transverse vibration					
calculated f, Hz	40.0	42.7	64.2	110	162
measured f, Hz	39	44	76	114	149

One can conclude that calculation of the characteristic parameters from the measured eigenvalues is a very effective tool for determining the tire characteristics. The natural frequencies describe the system much more accurately than is done by measurements of static deformation. The example of vibration of the belted tire showed that the theory developed allows a rational prediction of mechanical properties.

7. Summary. In this paper the mechanical characteristics of the belted tire are modeled using the circular beam under internal pressure on an elastic foundation. To demonstrate the validity of the assumption that the belt can be handled like a ring, the belt elastic properties are investigated experimentally and analytically. It appears that the steel-cord plies transmit the forces resulting from the deformations. Along the boundaries the steel wires carry forces to the surrounding rubber. In the layer between the oblique reinforcement very large shear deflections in the rubber arise. This phenomenon is restricted to a region near the boundary, so that the elastic properties of the belt can be calculated using a reduced width of the belt, like those of a reinforced beam.

The elastic stiffnesses are determined neglecting the circumferential curvature of the radially-reinforced side membrane. After that the equations of motion for this model are derived for the tire at rest as well as for the rotating tire. To illustrate the application of these equations three examples are worked out: (a) the static properties under side loads, (b) vibrations under vertical disturbances, (c) the formation of stationary waves at high rolling speeds.

To check the theory the radial and axial vibration characteristics of a Michelin-X-135-13 tire have been measured. The tire belt characteristics were calculated from the natural frequencies and compared with those obtained from the dimensions of the tire. They agreed satisfactorily, so that the model of the belted tire on which the theory is based is technically useful.

Literature

[1] B. J. Hinton, Investigation of tread band deformation under point lateral load. Diploma Thesis No. 61/2, Advanced School of Automobile Engineering, Cranfield, Bedfordshire, Engl. (1961).

[2] W. Borgmann, Theoretische und experimentelle Untersuchungen an Luftreifen bei Schräglauf. Dissertation an der Technischen Hochschule Braunschweig, 1963.

[3] F. Frank, Theorie des Reifenschräglaufs. Der Fakultät für Elektrotechnik der TH Darmstadt vorgelegte Dissertation, April 1965.

[4] K. Federhofer, Dynamik des Bogentägers und Kreisringes, Wien, 1956.

[5] E. Volterra, J. Appl. Mech., June 1953, p. 227.

[6] D. A. Rodriguez, J. Appl. Mech., Sept. 1961, p. 461.

[7] F. Martin, Theoretische Untersuchungen zur Frage des Spannungszustandes im Luftreifen bei Abplattung. Jahrbuch der deutschen Luftfahrtforschung I (1939), S. 490.

[8] R. B. Day and S. D. Gehman, Theory for the Meridian Section of Inflated Cord Tires, Rubber Chemistry and Technology 1963, S. 19.

[9] J. Rotta, Ing.-Arch. 17 (1949), S. 129.

[10] A. Chiesa, L. Oberto, and L. Tamburin, Transmission of Type Vibrations. Autom. Eng., Dec. 1964, p. 520.

Author's address: Dr. techn. Friedrich Böhm
7 Stuttgart-Uhlbach,
Innsbrucker Str. 73